A Study of a Čerenkov Photon Generator on the ^{16}N Calibration Source During the Airfill

Colin Okada
Lawrence Berkeley National Laboratory

SNO-STR-97-017

March 6, 1998

Abstract

An acrylic cylinder surrounding the ^{16}N calibration source may be used during the airfill period as a means of generating Čerenkov photons in main body of the Sudbury Neutrino Observatory. The use of this addition to the source could provide a way to test our ability to calibrate the PMTs and reconstruct positions within the detector.

1 Introduction

The Sudbury Neutrino Observatory (SNO) is a water Čerenkov detector which is being built to measure the flux and spectrum of the neutrinos coming from the Sun. In order to accomplish this, high confidence in the abilities of the hardware and software is necessary. This note presents one way in which we can test the combined output of these elements of the experiment prior to filling the detector with water.

The time shortly after the closing of the SNO cavity is expected to be used as a shakedown period for the detector. It is envisioned that during this time, the photo-multiplier tubes (PMTs), the data acquisition electronics, and the calibration sources will be tested to insure that both the hardware and software are in good working condition and ready for data accumulation and analysis. One potential short-coming in the current plans for the detector during this period may be the inability to have real events consisting of Čerenkov photons which can be used to perform a thorough test of the experiment from the accumulation of the data through the reconstruction of positions in the detector. One simple way of addressing this problem is to place the ^{16}N calibration source in an acrylic sleeve.

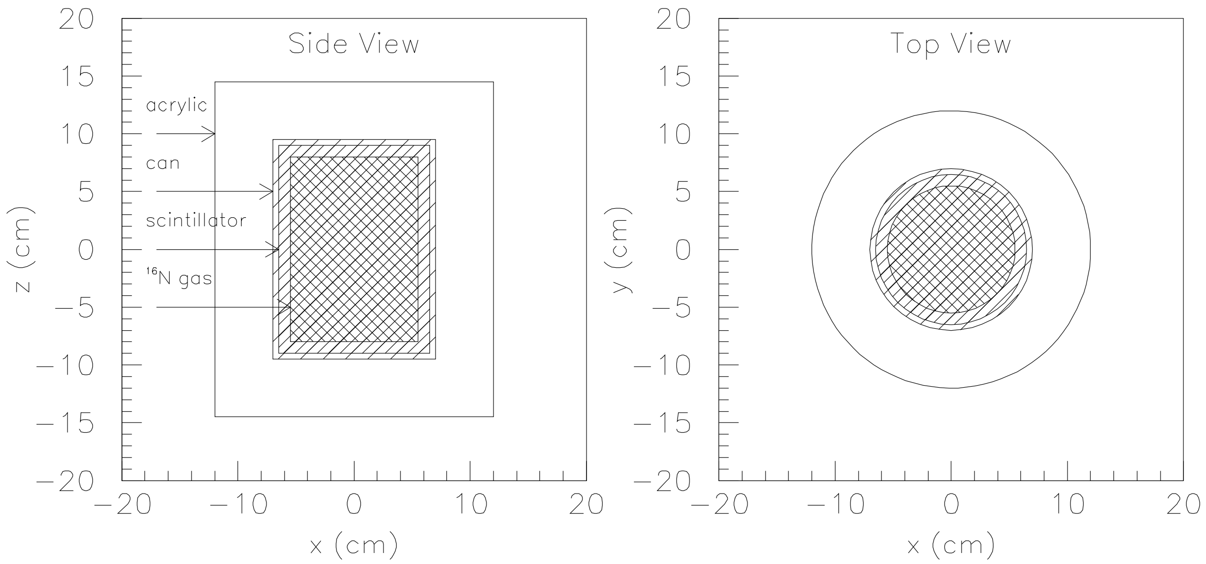

Figure 1: A sketch of the modified ^{16}N calibration source showing it encased in an acrylic cylinder.

2 Detector Design

In normal operations of the ^{16}N calibration source, γ-rays emerging from the source will be converted, via Compton scattering, to electrons, with these electrons generating Čerenkov light as they move through the heavy water (D_2O) of the SNO detector. During the period of the airfill, however, the absence of the D_2O will result in a much lower event rate. Only those γ-rays which are converted in the acrylic vessel (AV) will lead to Čerenkov light. Events resulting from conversions in the AV can be used to test the abilities of the fitting software, but, because the events will be generated only in a shell at the edge of what will be the D_2O volume, this only tests the software for a very specific event geometry.

The ^{16}N source can be modified to be a ready source of Čerenkov photons by enclosing it in a cylinder of acrylic. The γ-rays from the ^{16}N $\beta\gamma$ decays may convert within the acrylic of the cylinder, thus causing the cylinder to become a Čerenkov Ring Imaging Device (CRID). A sketch of the modified source is shown in Figure 1. Although the sketch shows a source encased in an acrylic volume, in the actual implementation of this idea, an acrylic jacket or sleeve placed around the ^{16}N source would be a more likely design. In this way, the device could be easily switched between the different modes of operation.

The events coming from data taken with the modified ^{16}N source can have calibration results applied to them and be passed to the event fitters so that vertices can be reconstructed. If the time calibrations are correct and the fitting algorithms are efficient, the results of the fits should be vertices at the ^{16}N source. Results dramatically different from this may be an indication of a problem with way the calibrations are performed. This scheme is more flexible and thorough than running with the unmodified source because of the vertex location will be well within the primary (D_2O) region of the detector. Also, because the source can be moved around the interior of the detector, the vertex finding software can be tested at several locations and a map of the fitting efficiency as a function of vertex position can be obtained.

3 Simulation Results

Simulations of the detector response to the modified ^{16}N source during the airfill have been carried out using SNOMAN. Different thicknesses for the acrylic cylinder have been tested to examine how this effects the performance. Table 1 shows the results for runs consisting of 10000 simulated ^{16}N $\beta\gamma$ decays with the airfill geometry, the ^{16}N source in the center of the detector, and different thicknesses for the CRID. The results for the total number of events with at least 10 PMT hits, and the numbers of those events in which the γ converted in either the AV or CRID are reported. An event is defined as having converted in the region if there is vertex containing an e^- or e^+ in the region. Results are also reported for simulated data without the CRID (0 cm) and in normal detector operation (water) for comparison. The number of events produced within the CRID increases with the thickness of the acrylic, and the event rate in the CRID matches the event rate in the AV for a cylinder thickness of about 3 cm. If this design change is implemented, a higher event rate in the CRID than in the AV will probably be desired, so a minimum thickness of $\sim$ 5 cm is suggested.

Looking closely at the case of the 5 cm acrylic cylinder, we can ask if the events being generated are useful in terms of the expected events with the fully operational SNO detector. Figure 2 shows the distribution of the number of PMTs hit for events with Čerenkov photons from the CRID or the AV. It is worth noting that the events coming from the CRID stop around 60 hits while the events coming from the AV stop around 30 hits. The difference in the end points of these distributions has been investigated. It has been determined that this comes about largely because the geometries of the CRID and AV lead to a higher probability for total internal reflection for Čerenkov photons produced in the acrylic vessel. Since the detector threshold for solar neutrino data is expected to correspond to approximately 50 hits, the CRID will provide a way of testing the detector and fitters around this threshold.

The events generated in the CRID and the AV were passed through the time fitter to see the effectiveness of the position reconstruction algorithm. The resulting distribution of difference between the fit position and the position of the electron is displayed in Figure 3. With this geometry, the difference between the positions peaks at $\sim$ 30 cm for the events coming from the CRID and $\sim$ 50 cm for events coming from the AV. Figure 4 shows how the ability to properly reconstruct an event is related to the number of PMT hits in the event by plotting the difference in position *vs.* the number of PMTs hit. From this it is seen that the fitting becomes very unreliable below about 30 PMT hits.

The effect of placing the calibration source at different locations in the detector has also been considered. The resulting event rates for the 5 cm thick acrylic cylinder at different the locations is shown in Table 2. Plots corresponding to the data taken at the different positions are shown in Figure 5 for the source at $z = 500$ cm, Figure 6 for the source at $z = 250$ cm, Figure 7 for the source at $z = -500$ cm, and Figure 8 for the source at $x = 500$ cm. Examination of these plots, shows that the fitting with the current algorithm will becomes somewhat less efficient the further the vertex is from the center of the detector. For all test locations away from the center, there is a broadening of the distribution for the position fit difference, and the peak of the distribution moves toward larger distances. The worst results occur when the vertex is directly under the hole at the top of the detector.

There was some concern expressed over this position dependence, so some additional tests utilizing different detector configurations were performed. In addition to the tests performed with the CRID during the airfill, photon bomb tests were done in SNO detectors filled with air and water. Figure 9 shows the difference in the position reconstruction for a photon bomb in air at the detector origin and at $z = 500$ cm where the effect in the CRID tests was the largest. There is some broadening of the distribution and a shift of the peak when the light is generated away from the center of the detector. Figure 10 shows the same test with a photon bomb in a detector filled with heavy water. Here there is almost no difference in the distributions. From these, we may conclude that the position dependence in the vertex reconstruction as shown by the CRID tests is a real effect, but that it will likely disappear when the detector is filled with water.

4 Discussion and Conclusions

A small modification to the ^{16}N calibration source has the potential of making the airfill period more interesting by producing the first Čerenkov photons within the main body of the detector. The amount of time used to run the calibration source has not yet been thought out, but, given the relatively high event rate expected from the ^{16}N source, it should take a rather short period of time to collect a sufficient amount of data. The proposed operation would be to run the calibration source at multiple locations both with and without the acrylic cylinder. By taking data without the CRID, information on the event rate, N_{hit} distribution, and fitting quality for events generated with the AV can be determined. This information can be used to characterize the events coming from the AV, and can be used to subtract the AV events from the data taken with the acrylic cylinder in place.

It is hoped that with this change to the ^{16}N source, the airfill detector becomes more than a place to test the operation of the hardware and some low level facets of the software for the SNO experiment. The airfill can be a laboratory in which the actual capability of the SNO detector and software can be examined through the reconstruction of events which are very close to the data expected during the full running of the detector. If necessary, the data with the modified source may be used to refine the event calibration and fitting routines. This may be especially interesting for events near the expected energy threshold for the detector.

In addition to the modified chamber described in this note, it has been suggested that a similar device consisting of an acrylic block surrounding a β source (^{90}Sr) may also be tried. This device would not be as effective because it would not able to provide an external trigger, and the lower energy of the β's will result in less light produced. However, it should be possible to make this second device smaller than the original one, thus allowing it to be dropped through one of the calibration tubes into the region between the acrylic vessel and the PMTs. This would extend the volume over which the detector can be tested by these Čerenkov photon devices.

Table 1: The total number of recorded events, and the number of events where the γ converted in the AV, CRID, or both the AV and CRID are reported for trials of 10000 $\beta\gamma$ events in ^{16}N with different thicknesses for the ^{16}N source cylinder. For comparison, the event rate for the calibration source in D_2O without the acrylic cylinder is also reported.

Thickness	Total	AV only	CRID only	AV & CRID
0 cm	489	489		
1 cm	617	440	82	97
2 cm	852	448	278	126
3 cm	980	403	413	164
4 cm	1096	368	537	191
5 cm	1281	381	718	182
water	6400			

Table 2: The results of simulation runs using the 5 cm thick acrylic cylinder with the source at different locations in the detector.

(x, y, z)	Total	AV only	CRID only	AV & CRID
$(0, 0, 500)$	1345	415	715	215
$(0, 0, 250)$	1296	390	683	223
$(0, 0, 0)$	1281	381	718	182
$(0, 0, -500)$	1412	479	673	260
$(500, 0, 0)$	1410	496	629	285

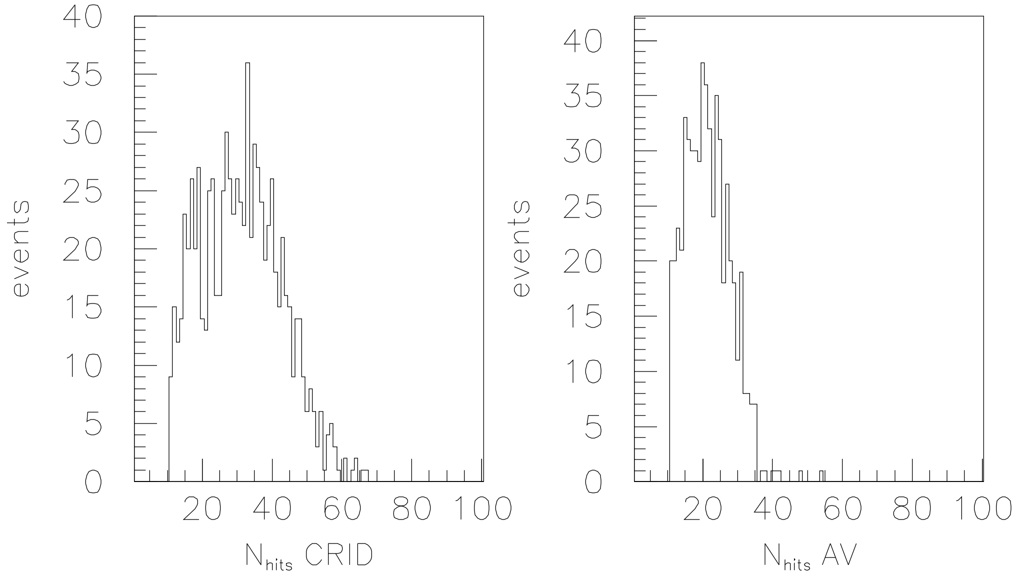

Figure 2: N_{hit} distribution for events with electrons only in the CRID and only in the AV for the case of a 5 cm cylinder thickness. The threshold for solar neutrinos is expected to be around $N_{hit} = 50$.

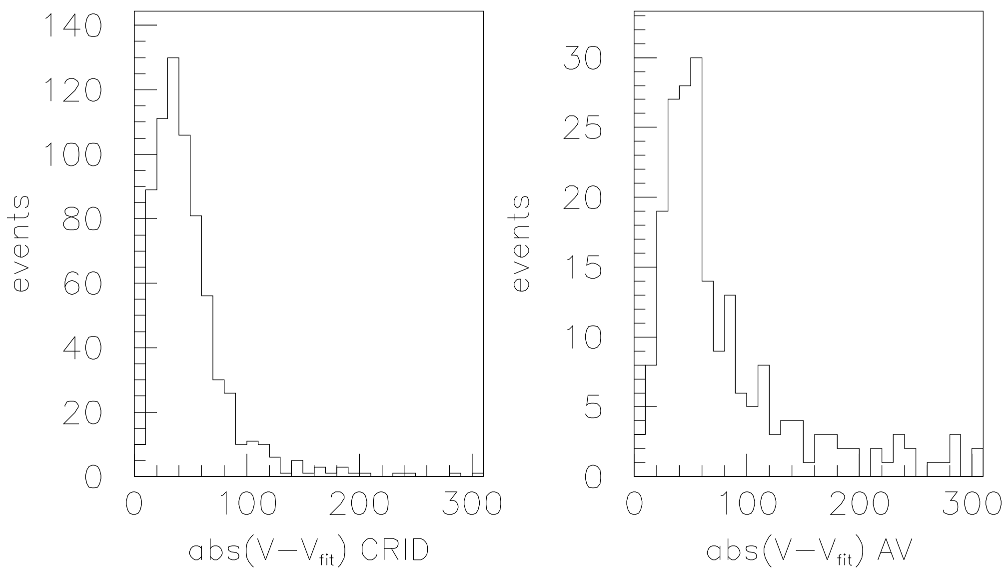

Figure 3: Distribution of the distance between the real vertex and the fit vertex (time fitter) for events with electrons only in the CRID and only in the AV for the case of a 5 cm cylinder thickness.

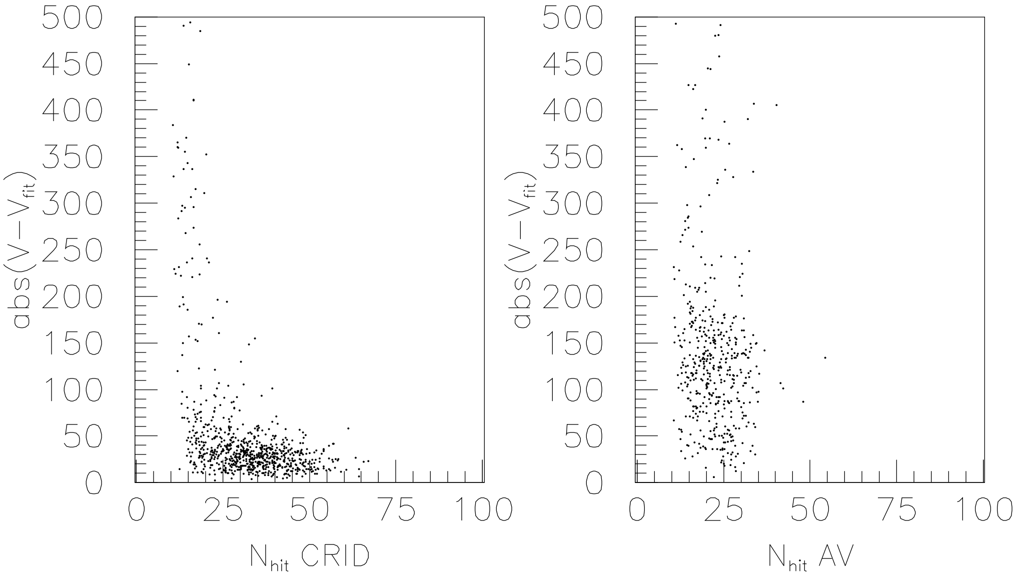

Figure 4: Distribution of the distance between the real vertex and the fit vertex (time fitter) *vs.* the number of PMT hits for events with electrons only in the CRID and only in the AV for the case of a 5 cm cylinder thickness. It seems the fitter becomes much worse for $N_{hit} < 30$.

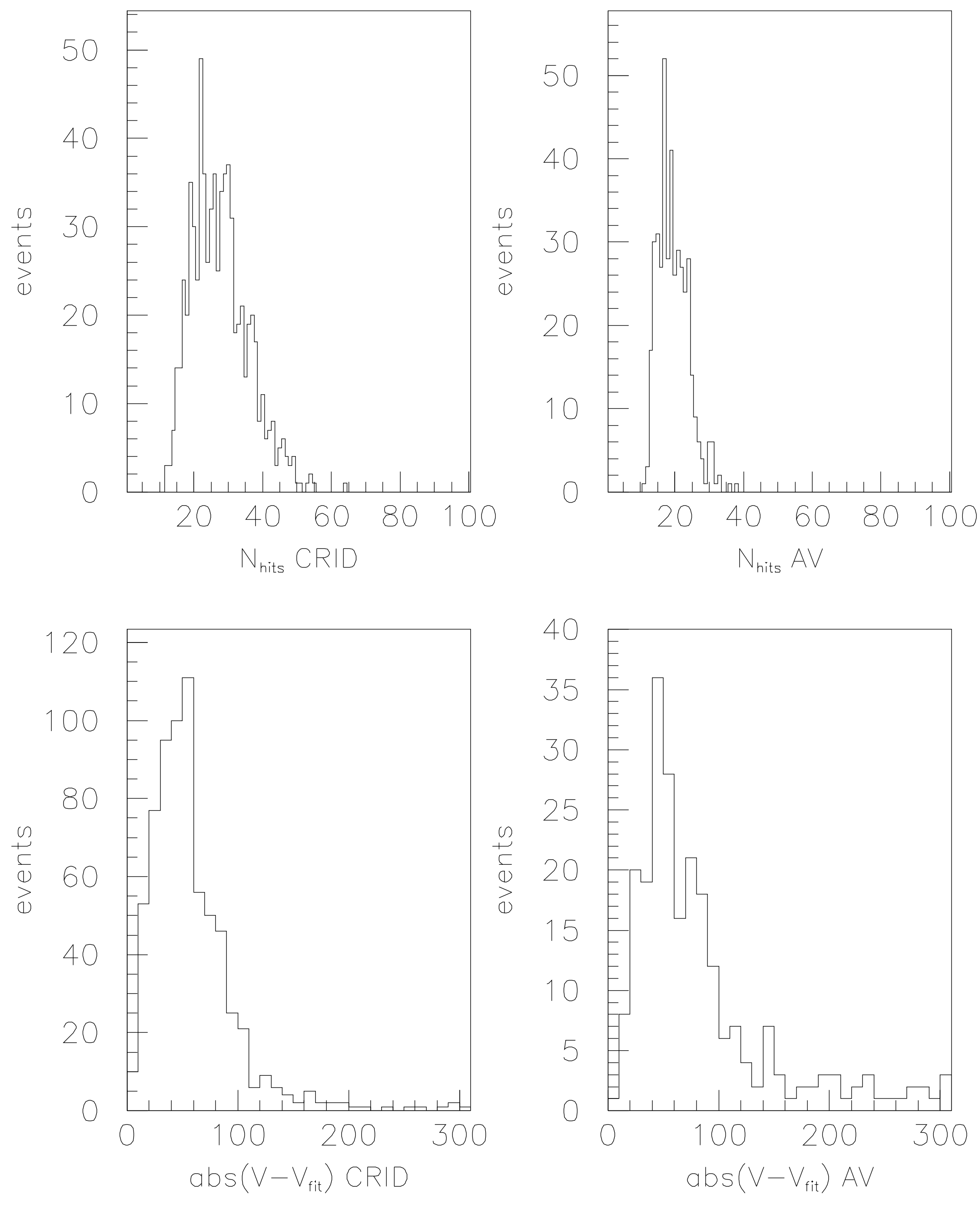

Figure 5: N_{hit} and reconstruction distance distributions for a 5 cm-thick CRID at $z = 500$ cm.

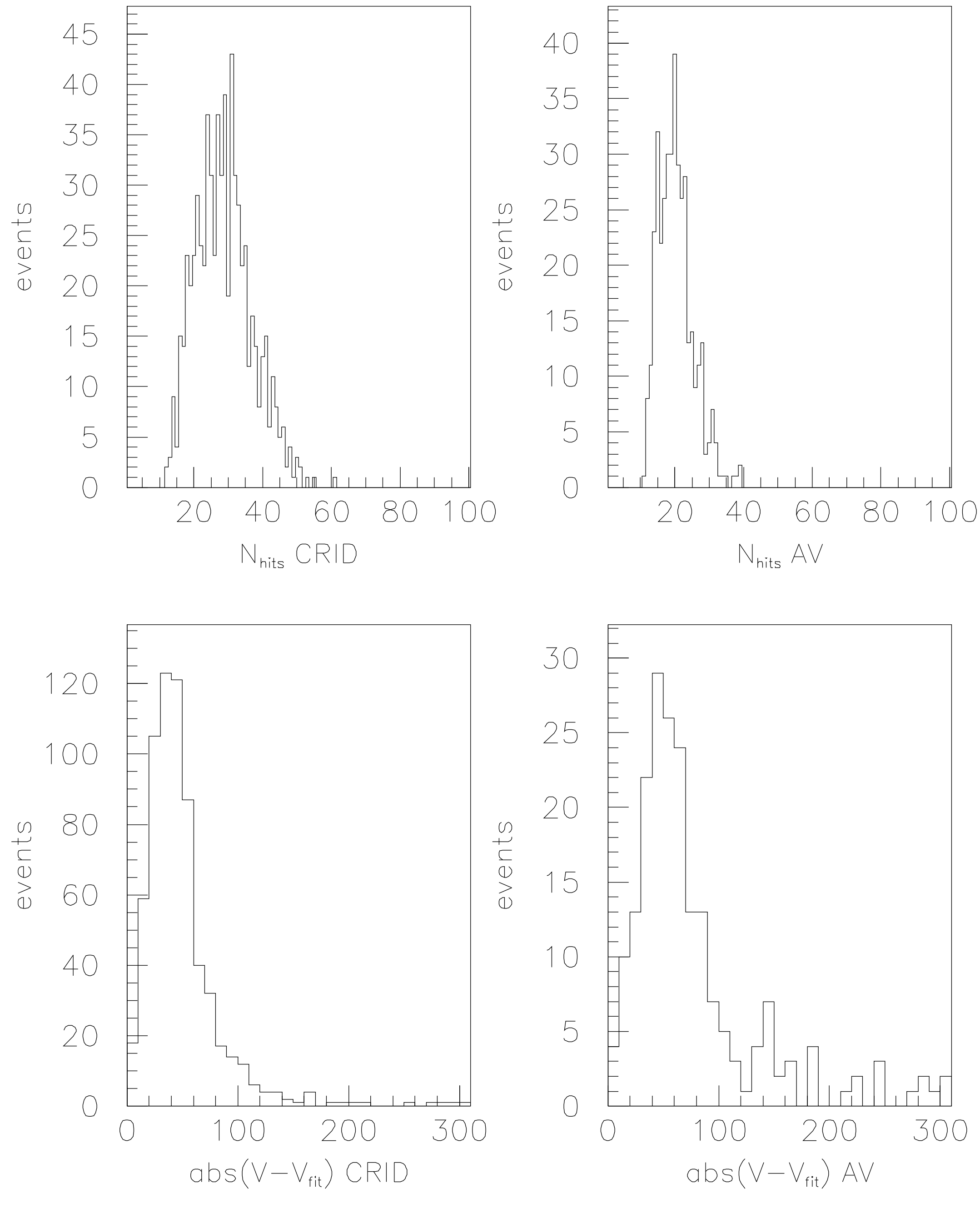

Figure 6: N_{hit} and reconstruction distance distributions for a 5 cm-thick CRID at $z = 250$ cm.

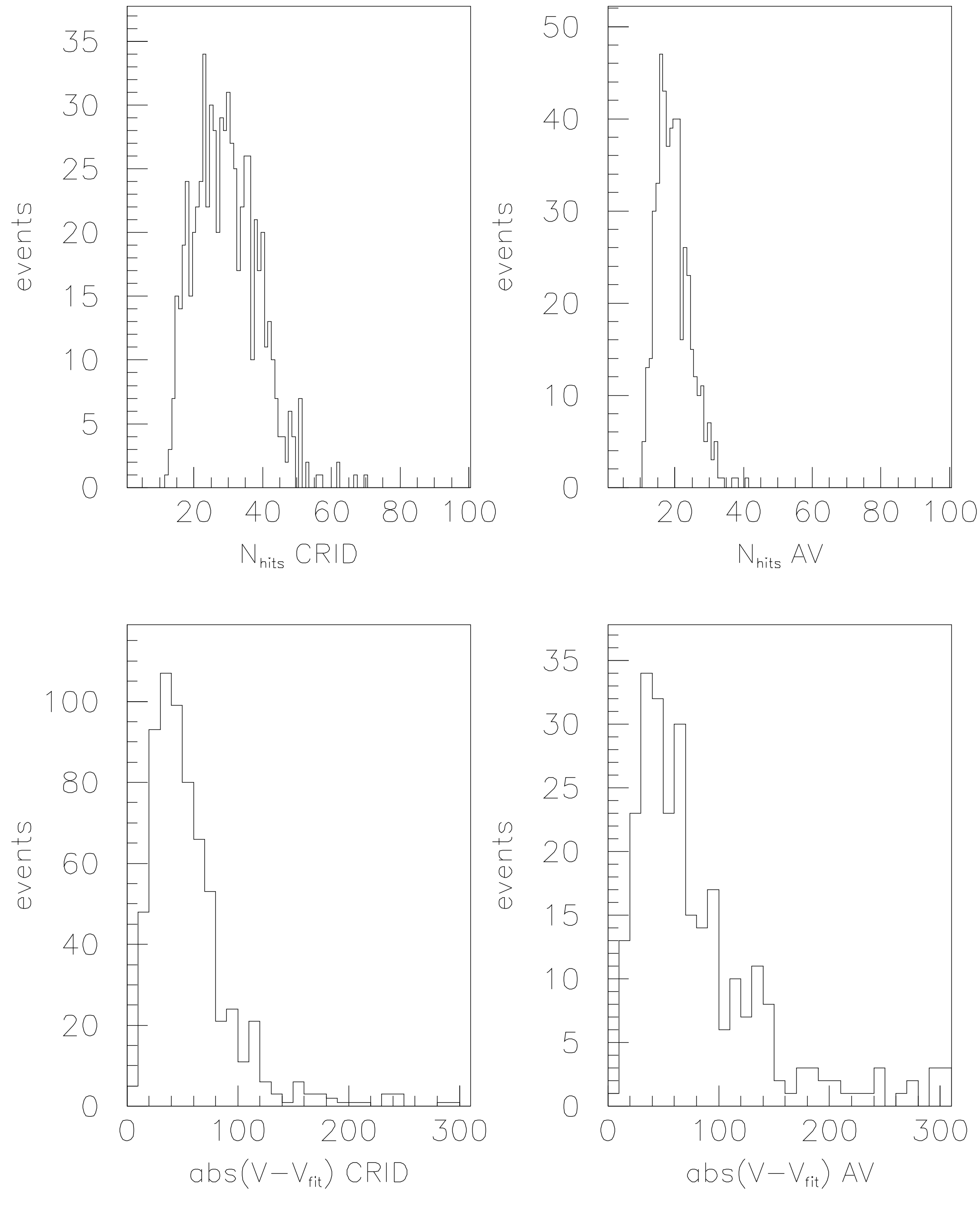

Figure 7: N_{hit} and reconstruction distance distributions for a 5 cm-thick CRID at $z = -500$ cm.

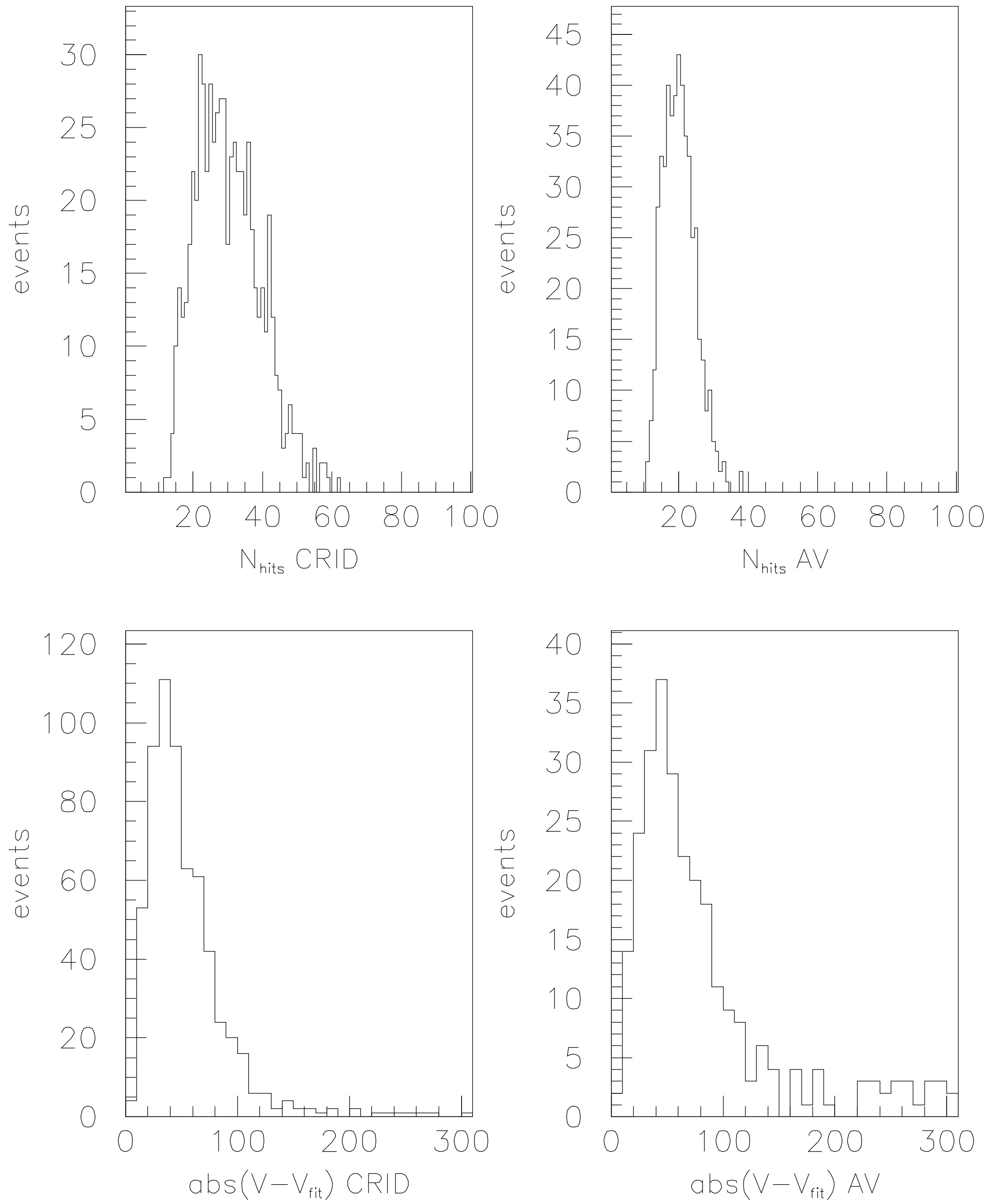

Figure 8: N_{hit} and reconstruction distance distributions for a 5 cm-thick CRID at $x = 500$ cm.

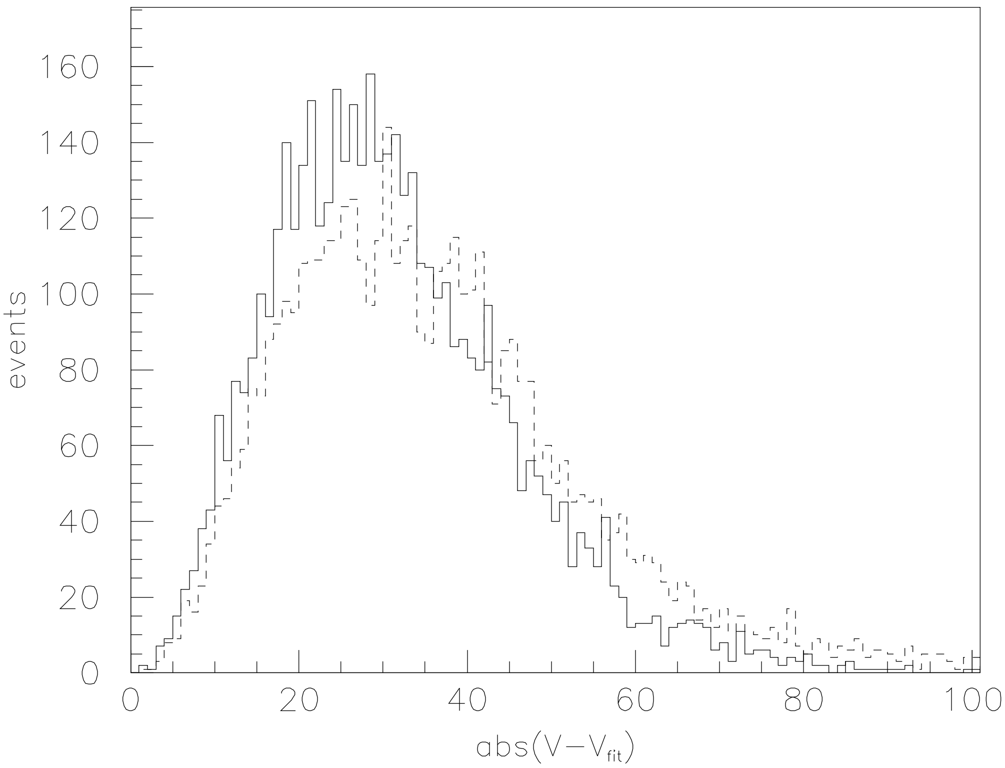

Figure 9: Reconstruction distance distributions for a photon bomb in air with the bomb located at the origin (full line) and at $z = 500$ cm (dashed line).

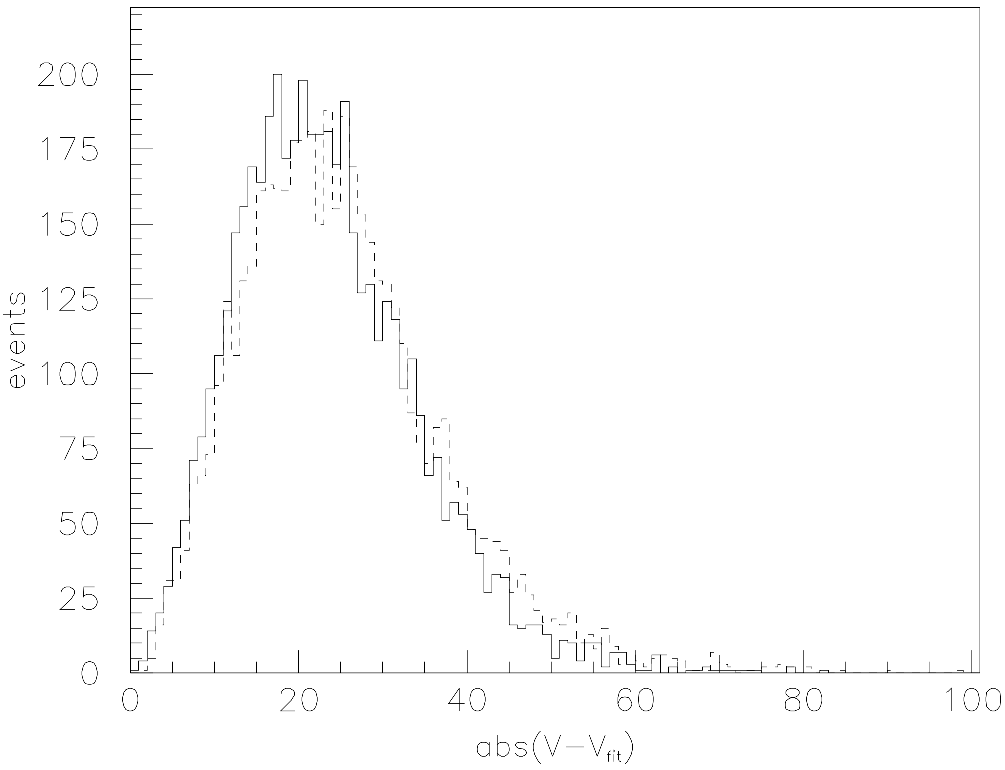

Figure 10: Reconstruction distance distributions for a photon bomb in water with the bomb located at the origin (full line) and at $z = 500$ cm (dashed line).